Chemical Mechanism of *Haemophilus influenzae* Diaminopimelate Epimerase†

Carolyn W. Koo and John S. Blanchard*

Department of Biochemistry, Albert Einstein College of Medicine, 1300 Morris Park Avenue, Bronx, New York 10461

Received December 10, 1998; Revised Manuscript Received February 11, 1999

ABSTRACT: Seven unique enzymatic steps lead to the biosynthesis of L-lysine from L-aspartate semialdehyde and pyruvate in bacteria. The immediate precursor to L-lysine is D,L-diaminopimelate, a diamino acid which is incorporated into the pentapeptide of the Gram-negative peptidoglycan moiety. D,L-Diaminopimelate is generated from the corresponding L,L-isomer by the *dapF*-encoded epimerase. Diaminopimelate epimerase is a representative of the pyridoxal phosphate-independent amino acid racemases, for which substantial evidence exists supporting the role of two cysteine residues as the catalytic acid and base. The pH dependencies of the maximum velocities in the L,L → D,L and D,L → L,L direction depend on a single catalytic group exhibiting p*K* values of 7.0 and 6.1, respectively, which must be unprotonated for activity. The pH dependencies of the *V*/*K* values in both directions depend on the ionization of two groups, one exhibiting a p*K* value of 6.7 which must be unprotonated and one exhibiting a p*K* value of 8.5 which must be protonated. Primary kinetic isotope effects on *V* and *V*/*K* are unequal, with $^{D}(V/K)$ being larger than ^{D}V in both the forward and reverse directions. Solvent kinetic isotope effects in both directions are inverse on *V*/*K*, but normal on *V*. Both of these isotopic observations support a model in which proton isomerization after catalysis and substrate dissociation is kinetically significant. A single solvent "overshoot" is observed when L,L-diaminopimelate is incubated with enzyme in D_2O; however, an unprecedented double overshoot is observed when D,L-diaminopimelate is incubated with enzyme in D_2O. A model has been developed which allows these two overshoots to be simulated. A chemical mechanism is proposed invoking the function of two cysteine residues, Cys73 and Cys217, observed in the recently determined three-dimensional structure of this enzyme [Cirilli, M., et al. (1998) *Biochemistry 37*, 16452−16458], as the acid and base in the mechanism.

The epimerization of L,L- to D,L-*meso*-diaminopimelate (DAP)[1] was first demonstrated by Work (*1*) in extracts of *Aerobacter aerogenes*, and the enzyme catalyzing this reaction, diaminopimelate epimerase (EC 5.1.1.7, Figure 1) was subsequently purified and characterized from *Escherichia coli* (*2*). The *dapF* gene, encoding DAP epimerase, was cloned and mapped in *E. coli* (*3*), and its sequence was reported the following year (*4*). The recombinant *E. coli* epimerase has been expressed, and shown to be stoichiometrically inactivated by an active site-directed aziridine derivative of diaminopimelate [aziDAP, 2-(4-amino-4-carboxybutyl)aziridine-2-carboxylate; *5*, *6*]. The irreversible inhibition of the epimerase by aziDAP is due to the alkylation of Cys73, suggesting that this residue is present at or near the active site (*5*).

Diaminopimelate epimerase is a member of the family of PLP-independent amino acid racemases. The racemization of amino acids is critical for providing substrates for the construction of bacterial peptidoglycan, which contains a number of D-amino acid centers, including D-glutamate, D-alanine, and D,L-diaminopimelate. The PLP-independent amino acid racemases have been subject to intense mechanistic scrutiny. The reactions catalyzed by bacterial proline racemase (*7*, *8*) and glutamate racemase (*9*, *10*) are notable in this regard, since both appear to operate by "two-base" mechanisms, and utilize a thiolate as the general base and a thiol as the general acid. While these two enzymes bear substantial mechanistic similarity, the active site thiols in proline racemase appear to be contributed by separate subunits of the 38 kDa dimer (*7*), whereas the active site thiols in glutamate racemase appear to be contributed by Cys73 and Cys184 of the same subunit of the 28.3 kDa monomeric enzyme (*9*). The three-dimensional structure of the *Haemophilus influenzae* diaminopimelate epimerase has recently been determined. The 274-amino acid monomeric

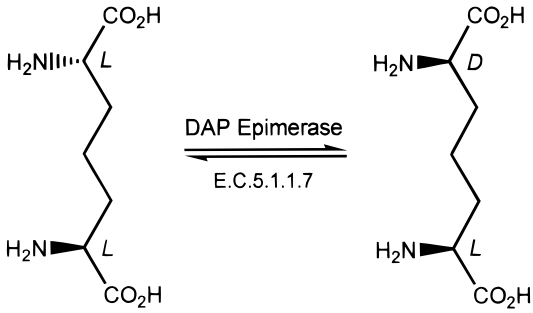

FIGURE 1: Reaction catalyzed by diaminopimelate epimerase.

† This work was supported by the National Institutes of Health (Grant AI33696).

* To whom correspondence should be addressed. E-mail: blanchar@aecom.yu.edu. Phone: (718) 430-3096. Fax: (718) 430-8565.

[1] Abbreviations: DAP, 2,6-diaminopimelic acid; aziDAP, 2-(4-carboxybutyl)aziridine-2-carboxylate; PLP, pyridoxal phosphate; NMR, nuclear magnetic resonance; ESI MS, electrospray ionization mass spectrometry; NADPH, β-nicotinamide adenine dinucleotide phosphate, reduced form; TEA, triethanolamine; DTT, dithiothreitol; CD, circular dichroism.

10.1021/bi982911f CCC: $18.00
Published on Web 03/19/1999

enzyme exhibits a novel, symmetric fold, in which two conserved cysteine residues, Cys73 and Cys217, are in disulfide linkage at the interface of two structurally superimposable domains (*11*).

A single mechanistic study of this unusual epimerase has been reported (*2*). This study suggested that diaminopimelate epimerase operates via a two-base mechanism, and that tritium incorporation into either the L,L- or D,L-diaminopimelates was accompanied by product formation, and was not the result of rapid exchange into substrate. We explore here a number of kinetic and isotopic approaches to better understand the mechanism of this reaction. The presence of two stereocenters in the substrate molecules, only one of which is catalytically interconverted, suggests a high degree of stereochemical stringency.

EXPERIMENTAL PROCEDURES

Materials. *H. influenzae* DAP epimerase and *Corynebacterium glutamicum meso*-DAP dehydrogenase were purified, as previously described, from *E. coli* BL21(DE3) cells containing expression vector pET23a(+)-*dapF* (*11*) or pET23a(+)-*dapdh* (*12*), respectively. A mixture of DAP isomers was purchased from Sigma, and the three stereoisomers of DAP (L,L, D,L, and D,D) were separated on a Chirobiotic T chiral column (250 mm × 10 mm, Advanced Separation Technologies Inc., Whippany, NJ) using a 70% aqueous methanol isocratic gradient on a Hewlett-Packard series 1100 HPLC apparatus. Dideuterated LL- and D,L-DAP were obtained by incubating commercial DAP in D_2O with DAP epimerase and separating the stereoisomers by HPLC (D,D-DAP did not incorporate deuterium). ^1H NMR was used to check the progress of deuterium incorporation, and electrospray mass spectrometry indicated 97 at. % excess deuterium in the purified dideuterated L,L- and D,L-DAP. Deuterium oxide (99.9 at. % excess) was purchased from Cambridge Isotope Laboratories (Andover, MA). Protein concentrations were determined by the Bio-Rad protein assay using bovine plasma γ-globulin as the standard.

Coupled Enzyme Assay for Diaminopimelate Epimerase Activity. During purification, DAP epimerase activity was assayed using *meso*-DAP dehydrogenase as a coupling enzyme. The L,L → D,L reaction was monitored by following NADPH production at 340 nm. Assays were performed in 20 mM TEA buffer (pH 7.8) with 1 mM DTT, 0.9 mM $NADP^+$, and 0.15 mM L,L-DAP.

Circular Dichroism Assay for Diaminopimelate Epimerase Activity. The activity of DAP epimerase was continuously monitored in both L,L → D,L and D,L → L,L on a Jasco J-720 spectropolarimeter. The molar ellipticity of L,L-DAP at 205 nm and pH 7.8 was determined to be 60.0 mdeg cm^{-1} mM^{-1} (D,L-DAP does not rotate polarized light). Assays were performed at 25 °C in phosphate or borate buffers containing 0.1 mM DTT to minimize spectropolarimetric interference.

pH Profiles. Enzyme activity was measured spectropolarimetrically over the pH range of 5.8−9.0 using either phosphate (5.8−7.7) or borate (7.9−9.0) as a buffer, and pH values were determined using an Accumet model 20 pH meter. Assays were performed at 25 °C in 50 mM buffer containing 0.1 mM DTT, and were initiated by the addition of enzyme. The kinetic parameters, V and V/K, were determined from duplicate determinations at five or six different substrate concentrations ranging from 0.2 to 3 mM at each pH value. The values of V and V/K were determined at each pH value using eq 1

$$v = VA/(K + A) \quad (1)$$

where V is the maximal velocity, A is the substrate concentration, and K is the Michaelis constant (K_m). The pK values associated with the ionization of groups influencing V or V/K were determined by fitting the data to eqs 2 and 3, respectively, using the Sigma Plot program (version 3.03, Jandel Scientific Software).

$$\log V = \log[C/(1 + H/K_a)] \quad (2)$$

$$\log V/K = \log[C/(1 + H/K_a + K_b/H)] \quad (3)$$

where C is the pH-independent plateau value, K_a is the ionization constant for the acidic group, K_b is the ionization constant for the basic group, and H is the hydrogen ion concentration.

Primary Deuterium and Solvent Kinetic Isotope Effects. Primary deuterium and solvent kinetic isotope effects on V and V/K were determined by spectropolarimetrically measuring the initial velocity of L,L- or D,L-DAP epimerization at various substrate concentrations with unlabeled or dideuterated DAP in H_2O, or unlabeled DAP in H_2O and D_2O. Each assay was conducted at 25 °C in buffer containing 50 mM K_2HPO_4 (pH 7.8) and 0.1 mM DTT. Primary and solvent deuterium kinetic isotope effects were calculated from eq 4 using the programs of Cleland (*13*).

$$v = VA/[K(1 + F_iE_{V/K}) + A(1 + F_iE_V)] \quad (4)$$

where F_i is the fraction of isotopic label (0.97 and 0.999, respectively) and $E_{V/K}$ and E_V are the isotope effects minus 1 on V/K and V, respectively.

D_2O Overshoots. Overshoot experiments were performed in 99.9% D_2O containing 3 mM substrate, 50 mM buffer, and 0.1 mM DTT and were initiated with enzyme. The ellipticity at 205 nm was followed with time until equilibrium was achieved. Control reactions were performed under similar conditions in H_2O and followed at 205 nm until the ellipticity remained constant. Simulations were performed using the Scientist program (MicroMath Scientific Software, Inc.).

RESULTS

Kinetic Constants. The kinetic constants were determined at pH 7.8. In the forward (L,L → D,L) direction, the k_{cat} was determined to be 128 ± 3 s^{-1}, and the K_m value of L,L-DAP was 0.7 ± 0.1 mM. In the reverse (D,L → L,L) direction, the k_{cat} was determined to be 82 ± 3 s^{-1}, and the K_m value of D,L-DAP was 1.1 ± 0.1 mM.

pH Profiles. The pH dependence of the maximum velocity for the conversion of L,L-DAP to D,L-DAP is dependent on the ionization of a single group whose protonation abolishes activity. The pK value of this group was determined to be 7.0 ± 0.1. Similarly, the pH dependence of the maximum velocity for the conversion of D,L-DAP to L,L-DAP is dependent on the ionization of a single group whose protonation abolishes activity. The pK value of this group was determined to be 6.1 ± 0.1. The pH-independent value

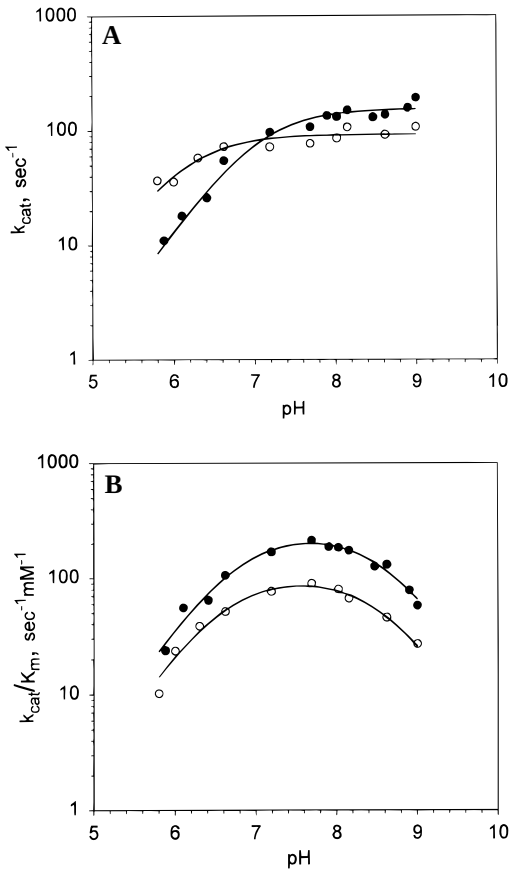

FIGURE 2: pH dependence of the maximum velocities (A) and *V*/*K* values (B) of L,L-DAP (○) and D,L-DAP (●). The points in the plots are experimentally determined, while the smooth lines are fits of the data to eqs 2 (A) and 3 (B).

Table 1: Kinetic Isotope Effects Exhibited by Diaminopimelate Epimerase

primary deuterium	^{D}V	$^{D}(V/K)$
L,L → D,L	2.5 ± 0.2	4.3 ± 0.7
D,L → L,L	4.3 ± 0.5	5.4 ± 1.1
solvent	^{D_2O}V	$^{D_2O}(V/K)$
L,L → D,L	1.8 ± 0.1	0.83 ± 0.08
D,L → L,L	1.5 ± 0.1	0.73 ± 0.09

of the maximum velocity for the conversion of L,L-DAP to D,L-DAP is approximately 2 times higher than that of the reverse reaction (Figure 2A). The pH dependencies of the *V*/*K* values for the two substrates are both bell-shaped, and yield statistically identical p*K* values of 6.7 and 8.5 for the two groups whose protonation and deprotonation, respectively, decrease the *V*/*K* values for the two substrates (Figure 2B).

Primary Deuterium Kinetic Isotope Effects. Primary deuterium kinetic isotope effects were determined under initial velocity conditions using dideuterated substrates, L_D,L_D- or D_DL_D-DAP. Under initial velocity conditions, larger isotope effects were observed on *V*/*K* [$^{D}(V/K)$] than on *V* (^{D}V) in both directions (Table 1). Further, the isotope effects were much larger in the reverse (D,L → L,L) direction than in the forward (L,L → D,L) direction. Thus, $^{D}V_{DL} = 4.3$, and $^{D}V_{LL} = 2.5$.

Solvent Kinetic Isotope Effects. Solvent kinetic isotope effects were determined under initial velocity conditions using protio-containing substrates. Nearly equivalent inverse solvent kinetic isotope effects on *V*/*K* were observed in both the forward and reverse directions, while nearly equivalent normal solvent kinetic isotope effects on *V* were observed in both the forward and reverse directions (Table 1).

D_2O Overshoots. The full time course of the enzymatic conversion of each substrate to the equilibrium mixture was determined in either H_2O or D_2O (Figure 3) by following the ellipticity change at 205 nm. In the reactions performed in H_2O in both directions, the ellipticity smoothly approached equilibrium. In the forward direction, a single "overshoot" was observed when the reaction was carried out in D_2O, where the concentration of D,L-DAP transiently exceeds its equilibrium concentration before returning to its equilibrium concentration. In the reverse direction, a "double overshoot" was observed, where the concentrations of L,L- and D,L-DAP transiently and consecutively exceed their equilibrium concentrations before attaining their final equilibrium concentrations. In both cases, the equilibrium constant ([D,L]/[L,L]) at infinite time was 2.0.

DISCUSSION

Diaminopimelate epimerase is a unique member of the family of PLP-independent amino acid racemases, containing two stereocenters in its diamino acid substrates. Due to the presence of these two centers, the equilibrium constant is 2, rather than 1, for all other racemases. While there may be minor enthalpic differences which contribute to the nonunitary equilibrium constant, the most likely explanation for the observed equilibrium constant is due to the entropic effect associated with interconverting the two stereocenters of L,L-DAP with the meso compound. Both proline and glutamate racemases catalyze similar reactions, and both have been shown, by alkylation and site-directed mutagenesis, to use two cysteine residues as the general base and acid, abstracting the Cα proton from one stereoisomer, and protonating the opposite face of the carbanionic intermediate or transition state, respectively. Diaminopimelate epimerase requires DTT for maximal activity, and an active site-directed irreversible inhibitor of the epimerase, [aziDAP, 2-(4-amino-4-carboxybutyl)aziridine-2-carboxylate; *5*, *6*] has been shown to stoichiometrically inactivate the *E. coli* enzyme. The irreversible inhibition of the epimerase by aziDAP is due to the alkylation of Cys73, suggesting that this residue is present at or near the active site (*5*). The corresponding residue in the *H. influenzae* enzyme is also Cys73, and is found in a disulfide linkage with Cys217 at the interdomain interface in the three-dimensional structure of the oxidized, crystallized enzyme (*11*).

pH Profiles. The pH dependencies of the *V*/*K* values for the two substrates are identical, as they must be, since the Haldane relationship requires that the ratio of the *V*/*K* values in the forward and reverse reaction must equal the equilibrium constant. The two bell-shaped profiles are thus displaced, and yield an experimental ratio of 2.4, close to the theoretical value of 2.0 for K_{eq}. Two groups are observed in the *V*/*K* profiles, and these reflect the ionization of free substrate or free enzyme groups. One, exhibiting a p*K* value of 6.7 ± 0.1, must be unprotonated, while the other, exhibiting a p*K* value of 8.5 ± 0.1, must be protonated. The p*K* values of diaminopimelate have been determined (1.8,

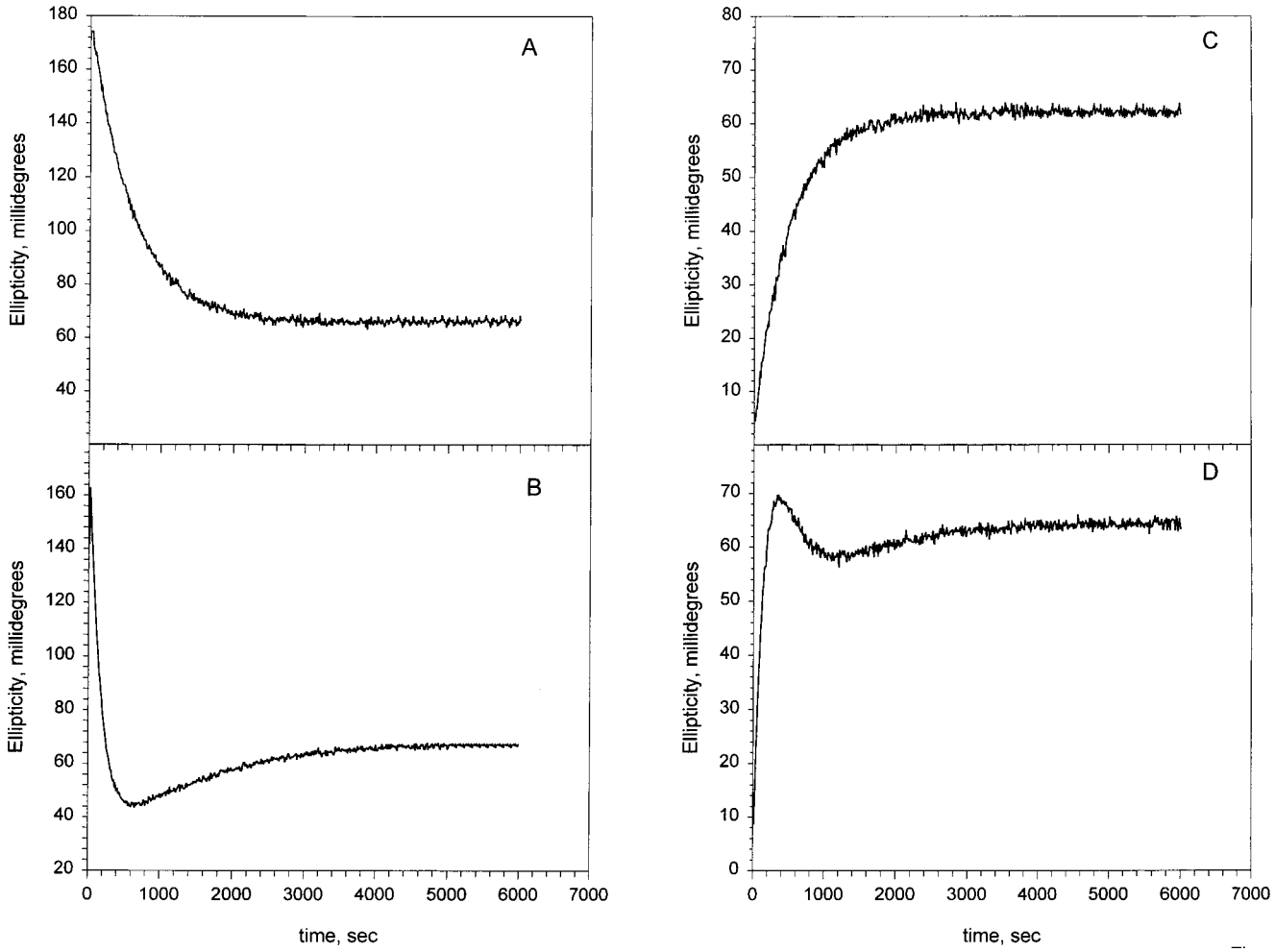

FIGURE 3: Time courses for conversion of L,L-DAP → D,L-DAP by diaminopimelate epimerase in H_2O (A) and D_2O (B) and D,L-DAP → L,L-DAP in H_2O (C) and D_2O (D) following the ellipticity change at 205 nm.

2.2, 8.8, and 9.9; *14*), and while the carboxylate p*K* values are too low to be observed, the α-amino group of the substrate is a possible candidate for the group exhibiting a p*K* value of 8.5. Alternatively, both groups observed in the *V*/*K* profiles may be the catalytic cysteine residues, one of which must be protonated to act as the general acid and the other of which must be unprotonated to act as the general base. The protonation states must be opposite in the two directions, however, suggesting that the identity of the two cysteines must be reversed in the two profiles. A similar bell-shaped pH dependence has been reported for the reaction of proline racemase (*15*).

In addition, in the reaction catalyzed by diaminopimelate epimerase, the enzyme must specifically recognize the L-stereocenter at the distal noncatalytic site, since the production of the D,D-isomer is never observed, and would have disastrous physiological consequences. There thus must be strong and specific interactions between the enzyme and the L-stereocenter of the substrates at the distal site. A number of candidate enzyme residues are appropriately positioned, and highly conserved among the 14 bacterial epimerase gene sequences, including K5, H7, and D12. Although obviously important in determining the stereoselectivity of the reaction, the ionization of the enzyme and substrate groups which provide these strong interactions apparently occurs outside of the pH region examined. Ultimately, the three-dimensional structure of an enzyme−substrate complex will be needed to clarify the identification of these groups.

The groups whose protonation abolishes the maximum velocities in either direction are assigned to the cysteine residues involved in the initial proton abstraction of the Cα proton from the proximal amino acid center. The macroscopic p*K* values determined for the two cysteines are 7.0 ± 0.1 in the forward direction and 6.1 ± 0.1 in the reverse direction. These p*K* values are those of the two cysteines in the E−L,L-DAP and E−D,L-DAP complexes, respectively, and are likely to be perturbed from their intrinsic values in the free enzyme. The protonated cysteine which acts as the general acid is not observed in the *V* pH profiles, suggesting that in the relevant enzyme−substrate complex, the p*K* has been elevated to a value of >9. This is likely the result of the desolvation of the protonated cysteine residue in the binary complex.

Kinetic Isotope Effects. The primary deuterium kinetic isotope effects are large in both directions, suggesting that chemistry is largely or partially rate-limiting, and that commitments to catalysis are low. Two features of the data presented in Table 1 are noteworthy. Both ^{D}V and $^{D}(V/K)$ are larger in the reverse direction than in the forward direction, and $^{D}(V/K)$ is larger than ^{D}V in both directions. The model shown in Figure 4 was used to derive the expressions for the primary deuterium kinetic isotope effects

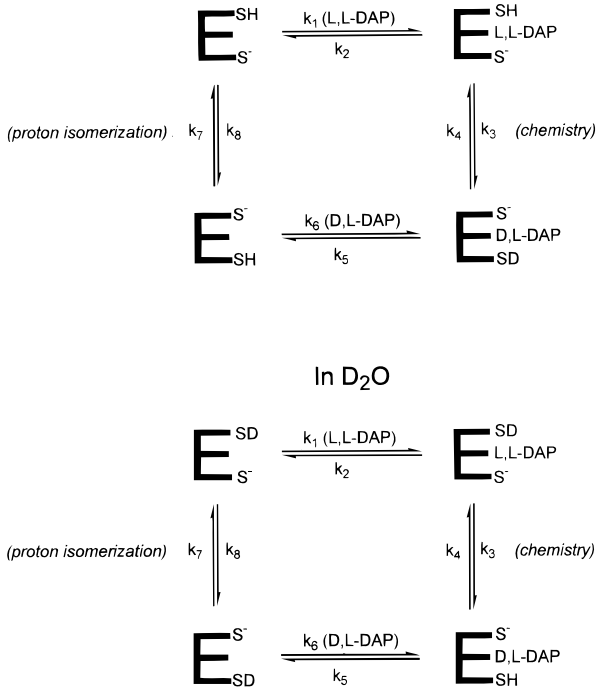

FIGURE 4: Model used to derive the expressions for the primary deuterium kinetic isotope effects.

shown below.

$$^{D}(V/K_{LL}) = (^{D}k_3 + k_3/k_2 + k_4/k_5{}^{D}K_{eq})/(1.0 + k_3/k_2 + k_4/k_5) \quad (5)$$

$$^{D}(V/K_{DL}) = (^{D}k_4 + k_4/k_5 + k_3/k_2{}^{D}K_{eq})/(1.0 + k_4/k_5 + k_3/k_2) \quad (6)$$

$$^{D}V_{LL} = [^{D}k_3 + k_3(1.0/k_5 + 1.0/k_7) + k_4/k_5{}^{D}K_{eq}]/[1.0 + k_3(1.0/k_5 + 1.0/k_7) + k_4/k_5] \quad (7)$$

$$^{D}V_{DL} = [^{D}k_4 + k_4(1.0/k_2 + 1.0/k_8) + k_3/k_2{}^{D}K_{eq}]/[1.0 + k_4(1.0/k_2 + 1.0/k_8) + k_3/k_2] \quad (8)$$

The ratio of the $^{D}(V/K)$ values for the D,L- and L,L-DAP is not 1, as reported for proline racemase (*8*). This suggests that the intrinsic primary deuterium kinetic isotope effects for the removal of the α-D- and α-L-protons are different. This suggestion is based on comparing eqs 5 and 6, the expressions for the *V*/*K* isotope effects in the two directions. The two expressions share the same denominator, and their ratio is simply the ratio of the two numerators. $^{D}K_{eq}$ is the same in both expressions (1.14; *16*) for transfer of the deuterium from the α-amino acid to water, and both commitment factors, k_3/k_2 and k_4/k_5, are likely to be small given the magnitude of the observed effects. The ratio of the observed *V*/*K* isotope effects thus reduces to the ratio of the intrinsic kinetic isotope effects for removal of the α-D- and α-L-protons by the two different cysteine residues. Similar differences in the apparent $^{T}(V/K)$ values observed in the two directions have been reported for DAP epimerase (*2*).

The observation that the determined values for ^{D}V are smaller than the determined values for $^{D}(V/K)$ in either direction suggests that an additional slow step, in addition to chemistry, is partially rate-limiting, and follows product

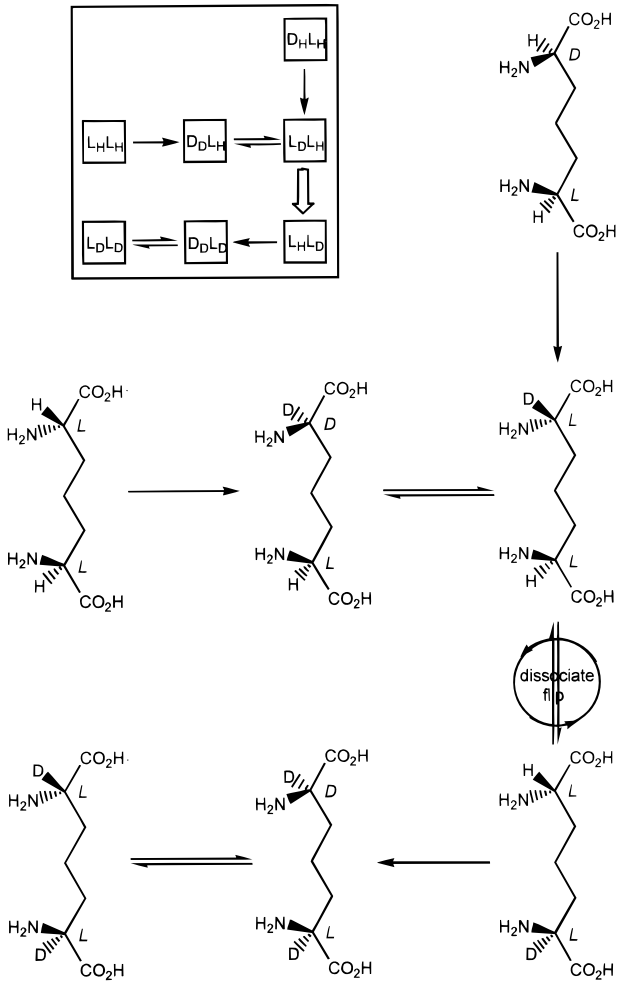

FIGURE 5: Protoisomers of DAP generated during the reactions of L,L-DAP (upper left) or D,L-DAP (upper right) in D_2O.

dissociation. The model shown in Figure 4 includes a proton isomerization from one cysteine residue, protonated at the end of the catalytic event but required to be unprotonated for subsequent turnovers, to the other cysteine residue, unprotonated at the end of the catalytic event but required to be protonated for subsequent turnovers. This prototrophic shift appears in the expressions for ^{D}V as the inclusion of the two rate constants, k_7 and k_8, in the expressions for ^{D}V for L,L- and D,L-DAP, respectively (eqs 7 and 8). If it is assumed that the observed $^{D}(V/K)$ values are equal to the intrinsic isotope effects in the two directions, and that only the k_3/k_7 or k_4/k_8 terms contribute significantly to the numerator, then values of 0.3−1 are obtained for the ratio of the catalytic step and prototrophic shift in both directions. This very simplified analysis argues that chemistry is only 1−3 times slower than the interconversion of the two singly protonated enzyme species. Similar slow intramolecular proton transfers have been documented previously for proline racemase (*17*) as well as for other enzymes (*18*, *19*).

Solvent Kinetic Isotope Effects. Additional support for this analysis comes from the solvent kinetic isotope effects (Table 1). The solvent kinetic isotope effects on *V*/*K* determined under initial velocity conditions for both substrates are inverse, providing additional evidence for the catalytic involvement of cysteine residues. The relevant fractionation factors are those of the substrate ($\Phi = 1.14$) and unprotonated thiolate anion, and the carbanion and protonated thiol

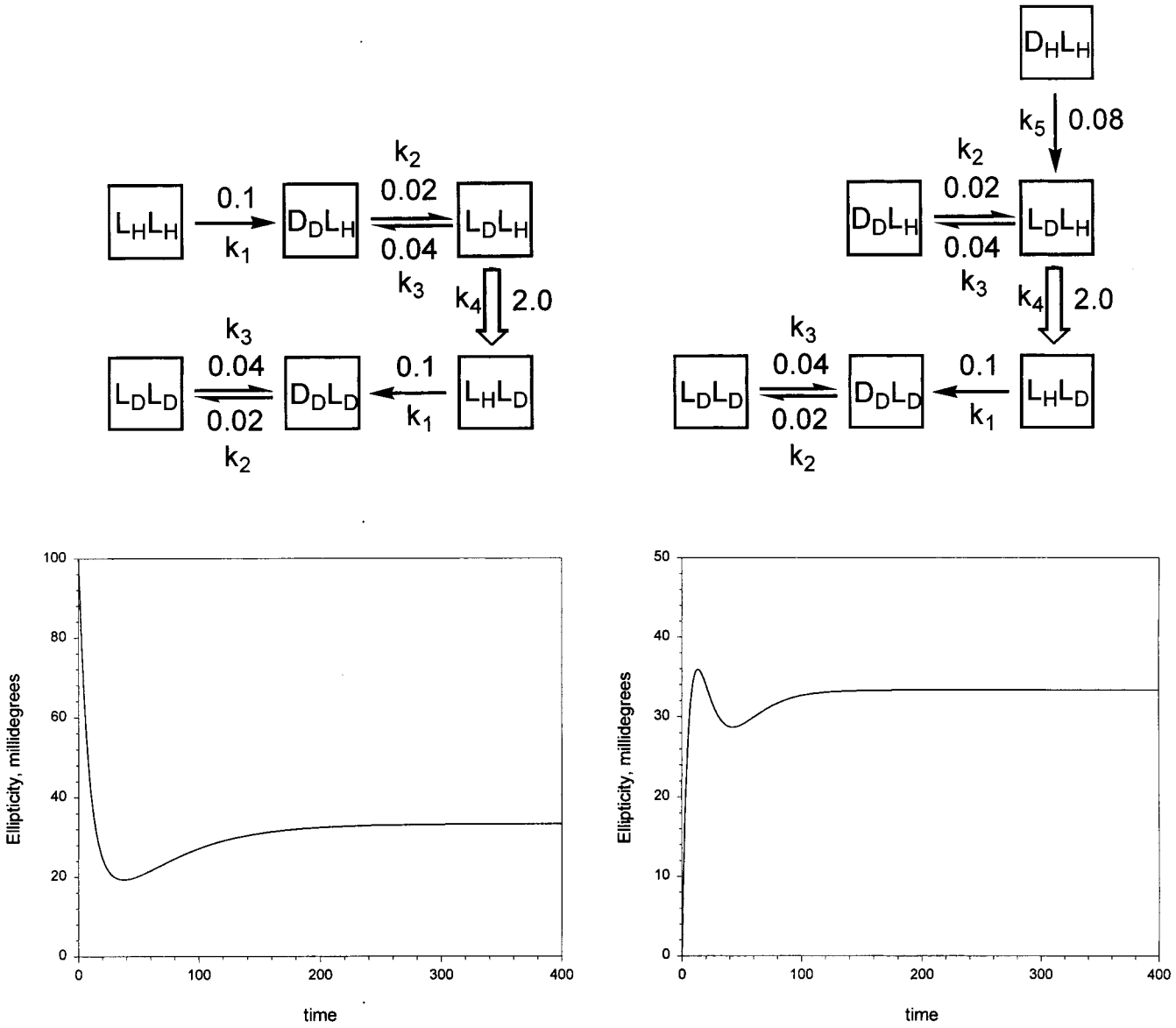

FIGURE 6: Models with rate constants used to simulate the D_2O overshoots. The models are shown in the upper portion, and the simulated time courses are shown below each model. Simulations were performed using the Scientist program (MicroMath Scientific Software, Inc.).

($\Phi \approx 0.4-0.6$; *8*). On the other hand, the solvent kinetic isotope effects on *V* are normal. The expressions for *V*, but not for *V*/*K*, include the rate constants associated with the prototrophic shift. As was suggested above, this step may be partially rate-limiting, and only 1−3 times faster than the catalytic step. A large solvent kinetic isotope effect on this step is certainly suggested by these data.

D_2O Overshoots. Equilibrium overshoots accompanying the racemization of amino acids in D_2O (*9*, *15*) and the more general observation of "equilibrium perturbations" (*20*) rely on the introduction or presence of a heavy isotope at a position at or near the chemically reactive center. Such overshoots and perturbations occur because of the slower, isotope-induced, attainment of isotopic equilibrium with respect to the bulk chemical equilibrium. In the case of proline racemase, the original observation of overshoots (*15*) was followed by a critical examination of the reaction mechanism by Knowles and co-workers (*21*, *22*). Subsequent work with glutamate racemase yielded similar results (*10*). The peculiarity, and uniqueness, of the diaminopimelate epimerase system arises from the presence of not one, but two, stereocenters in the two substrates.

When the conversion of L,L-DAP to the equilibrium mixture containing 33% L,L-DAP and 66% D,L-DAP is followed in H_2O, no overshoot is observed. When this same experiment is performed in D_2O, a single overshoot is observed. Similarly, when the conversion of D,L-DAP to the equilibrium mixture containing 33% L,L-DAP and 66% D,L-DAP is followed in H_2O, no overshoot is observed. However, when this experiment is performed in D_2O, an unprecedented double overshoot is reproducibly observed. Although the appearance of a double overshoot is not possible for the reactions catalyzed by proline or glutamate racemase, we posited that the added kinetic complexity of the epimerization of DAP might be responsible for this result. As shown in Figure 5, seven of the eight possible non-, mono-, and dideuterated DAP complexes are transiently generated during these reactions (the D_HL_D cannot be formed, and while the L_HL_D and L_DL_H are equivalent in solution, binding to the enzyme generates the nonequivalence), with the final prod-

ucts being the dideuterated DAPs, L_DL_D and D_DL_D. Three types of steps are shown in the figure: irreversible steps occurring during washin of deuterium from D_2O, interconversion of a deuterated L- or D-center with a deuterated D- or L-center, and finally the dissociation/reassociation reaction interconverting bound L_HL_D and L_DL_H. The first of these steps was considered to be fast, on the basis of the observations of inverse *V*/*K* solvent kinetic isotope effects. The second of these was considered to be slow, and nonequivalent, on the basis of the observations of different, and large, primary deuterium kinetic isotope effects. The dissociation/reassociation steps were considered to be the fastest, since no isotopic evidence implicates kinetically important product dissociation, and no prototrophic shifts are required in the interconversion of L_HL_D and L_DL_H. The two overshoot reactions were simulated using the models shown in Figure 6 (top) and using the same rate constants for the steps for both simulations. The symmetry of the model requires that many of the steps, or ratios of steps, be fixed. Thus, the observed equilibrium constant of 2 requires that the ratio k_3/k_2 be equal to 2. These rate constants are present in both the upper "arm" of the model, and in the lower "arm" since both reactions interconvert a deuterated L- and deuterated D-stereocenter. The difference is simply whether the distal L-stereocenter is protonated or deuterated. Similarly, the rate constant for washin of deuterium into the L-stereocenter is not affected by the presence of deuterium in the distal L-center. The results of the simulations are qualitatively compelling; starting with L,L-DAP, only a single overshoot is simulated, while starting with D,L-DAP, a double overshoot is simulated (Figure 6, bottom). There are likely to be a number of numerically different possibilities for the simulations, but the appearance of the double overshoot is due to the different isotope effects observed in the two different directions. Starting with D_HL_H, the initial rapid formation of L_DL_H is followed by a branch, in which this molecule can dissociate or more slowly react, via k_3, to generate the D_DL_H species. This is only converted back to L_DL_H by an even slower step, k_2, resulting in an isotopically induced kinetic "trap". This results in the appearance of the first of the two overshoots. The second overshoot is the result of the final equilibration of dideuterated DAPs. The double overshoot does not appear starting with L,L, since the kinetic trap experienced when starting with the D,L-isomer is not encountered, due to the slower reaction in this direction.

To validate the double overshoot simulations, we held k_3 and k_2 constant at 0.04 and 0.02, respectively, and individually varied k_1, k_4, and k_5. At k_1 values of >0.15, the first overshoot appears below the final equilibrium position, while at k_1 values of <0.04 (where there is no isotope effect in the L,L $\rightarrow$ D,L direction), only a single overshoot is observed. At k_5 values of <0.07, the first overshoot appears below the final equilibrium position; however, if $k_5 < 0.02$ (where there is no isotope effect in the D,L $\rightarrow$ L,L direction), no overshoots are observed. Decreases in k_4 below the value reported in Figure 6 maintain the double overshoot, but incrementally cause the initial overshoot to become greater. The ratio of the rate constants thus appears to be highly constrained to allow for the reproduction of the experimental results. These simulations suggest that the isotope effects in both directions (k_1/k_3 and k_5/k_2) are different and that the isotope effect in the D,L $\rightarrow$ L,L direction must be sufficiently larger than in the L,L $\rightarrow$ D,L direction for a double overshoot.

In conclusion, while being obviously similar to other amino acid racemases, DAP epimerase exhibits a number of unique properties not previously seen with other PLP-independent racemases. These include a nonunitary value for the equilibrium constant, dissimilar primary kinetic isotope effects in the two directions, and the unprecedented observation of a double overshoot in the D,L $\rightarrow$ L,L direction. Simple kinetic models and simulations have been used to quantitatively analyze these data. The remaining question of which of the two active site cysteines is responsible for proton abstraction from the two enantiomeric Cα−H bonds is currently under investigation.

ACKNOWLEDGMENT

We thank W. W. Cleland for his careful reading of the manuscript and suggestions and Edward Nieves of the AECOM Laboratory for Macromolecular Analysis.

REFERENCES

1. Antia, M., Hoare, D. S., and Work, E. (1957) *Biochem. J. 65*, 448−459.
2. Wiseman, J. S., and Nichols, J. S. (1984) *J. Biol. Chem. 259*, 8907−8914.
3. Richaud, C., Higgins, W., Mengin-Lecreulx, D., and Stragier, P. (1987) *J. Bacteriol. 169*, 1454−1459.
4. Richaud, C., and Printz, C. (1989) *Nucleic Acids Res. 16*, 10367.
5. Higgins, W., Tardif, C., Richaud, C., Krivanek, M. A., and Cardin, A. (1989) *Eur. J. Biochem. 186*, 137−145.
6. Gerhart, F., Higgins, W., Tardif, C., and Ducep, J.-B. (1990) *J. Med. Chem. 33*, 2157−2162.
7. Rudnick, G., and Abeles, R. H. (1975) *Biochemistry 14*, 4515−4522.
8. Belasco, J. G., Albery, W. J., and Knowles, J. R. (1986) *Biochemistry 25*, 2552−2558.
9. Gallo, K. A., and Knowles, J. R. (1993) *Biochemistry 32*, 3981−3990.
10. Tanner, M. E., Gallo, K. A., and Knowles, J. R. (1993) *Biochemistry 32*, 3998−4006.
11. Cirilli, M., Zheng, R., Scapin, G., and Blanchard, J. S. (1998) *Biochemistry 37*, 16452−16458.
12. Reddy, S. R., Scapin, G., and Blanchard, J. S. (1996) *Proteins: Struct., Funct., Genet. 25*, 514−516.
13. Cleland, W. W. (1979) *Methods Enzymol. 78*, 103−138.
14. Work, E. (1963) *Methods Enzymol. 6*, 624−634.
15. Cardinale, G., and Abeles, R. H. (1968) *Biochemistry 7*, 3970−3978.
16. Cook, P. F., Blanchard, J. S., and Cleland, W. W. (1980) *Biochemistry 19*, 4853−4858.
17. Fisher, L. M., Albery, W. J., and Knowles, J. R. (1986) *Biochemistry 25*, 2538−2542.
18. Rose, I. A., Warms, J. V., and Kuo, D. J. (1992) *Biochemistry 31*, 9993−9999.
19. Northrop, D. B., and Rebholz, K. L. (1997) *Arch. Biochem. Biophys. 342*, 317−321.
20. Schimerlik, M. I., Rife, J. E., and Cleland, W. W. (1975) *Biochemistry 14*, 5347−5353.
21. Fisher, L. M., Belasco, J. G., Bruice, T. W., Albery, W. J., and Knowles, J. R. (1986) *Biochemistry 25*, 2543−2551.
22. Albery, W. J., and Knowles, J. R. (1986) *Biochemistry 25*, 2572−2577.

BI982911F